

# Monitoring Vibrations on the Jefferson City Truss Bridge



Prepared by  
Glenn Washer  
Pedro Ruiz Fabian  
James Dawson  
Department of Civil and Environmental Engineering, University of Missouri-  
Columbia



Final Report Prepared for Missouri Department of Transportation  
May 2016

Project TR201605

Report cmr16-012

## TECHNICAL REPORT DOCUMENTATION PAGE

<b>1. Report No.</b> cmr 16-012	<b>2. Government Accession No.</b>	<b>3. Recipient's Catalog No.</b>	
<b>4. Title and Subtitle</b> Monitoring Vibrations on the Jefferson City Truss Bridge		<b>5. Report Date</b> May 25, 2016 Published: May 2016	
<b>7. Author(s)</b> Glenn Washer, Pedro Ruiz Fabian, James Dawson		<b>6. Performing Organization Code</b>	
<b>9. Performing Organization Name and Address</b> Department of Civil and Environmental Engineering University of Missouri-Columbia E2509 Lafferre Hall, Columbia, MO 65201		<b>8. Performing Organization Report No.</b>	
<b>12. Sponsoring Agency Name and Address</b> Missouri Department of Transportation (SPR) <a href="http://dx.doi.org/10.13039/100007251">http://dx.doi.org/10.13039/100007251</a> Construction and Materials Division P.O. Box 270 Jefferson City, MO 65102		<b>10. Work Unit No.</b>	
		<b>11. Contract or Grant No.</b> MoDOT project #TR201605	
		<b>13. Type of Report and Period Covered</b> Final Report (August 2015-February 2016)	
		<b>14. Sponsoring Agency Code</b>	
<b>15. Supplementary Notes</b> Project title: Monitoring Vibrations on the JC Truss Bridge. Conducted in cooperation with the U.S. Department of Transportation, Federal Highway Administration. MoDOT research reports are available in the Innovation Library at <a href="http://www.modot.org/services/or/byDate.htm">http://www.modot.org/services/or/byDate.htm</a> . This report is available at <a href="https://library.modot.mo.gov/RDT/reports/TR201605/">https://library.modot.mo.gov/RDT/reports/TR201605/</a> .			
<b>16. Abstract</b> The objective of the research was to determine the frequency and cause of resonant vibrations of truss verticals on bridge A4497 over the Missouri River in Jefferson City, MO. Instrumentation to monitor the vibrations of four verticals was installed on the bridge and monitored for 42 days. The instrumentation consisted of wireless accelerometers that monitored the accelerations on the four verticals. Weather data available from a weather station located at the Jefferson City Airport was used to analyze the weather conditions causing resonant vibrations of the verticals. It was found that there were eleven vibration "events" in which the vertical members vibrated with higher than normal accelerations. The average wind speeds during the events was about 17 mph. The wind direction during the events was from the WNW/NW during nine of the "events" and from the SE for 2 of the "events." It was found that the frequency of the events was 0.26 events per day during the monitoring period.  Historical weather data was analyzed to determine how frequently the resonance vibrations may be occurring, i.e., how frequently the combined wind speed and direction matched the conditions determined through the field monitoring. Historical weather data from 442 days was analyzed and it was found that there were 89 occurrences of the combined wind speed and direction that could cause vibrations of the vertical members. The resulting frequency of events was determined to be 0.20 events per day.  It was concluded that the frequency of resonant vibration events is likely 0.25 events per day or less. The vibrations are caused by average winds from the WNW/NW or SW of ~17 mph or greater, based on monitoring results. Recommendations stemming from the research were as follows: 1) The effect of the vibration events on the durability of the members should be analyzed further to determine if a retrofit is necessary. The data provided through the field monitoring should be used in the analysis; and 2) Other vertical members of a similar length should be monitored to determine if they are affected by resonant vibrations.			
<b>17. Key Words</b> Data analysis; Resonance frequency; Truss bridges; Trusses; Vertical supports; Vibration; Weather conditions		<b>18. Distribution Statement</b> No restrictions. This document is available through the National Technical Information Service, Springfield, VA 22161.	
<b>19. Security Classif. (of this report)</b> Unclassified.	<b>20. Security Classif. (of this page)</b> Unclassified.	<b>21. No. of Pages</b> 43	<b>22. Price</b>

# **Monitoring Vibrations on the JC Truss Bridge**

## **FINAL REPORT**

Prepared By:  
Glenn Washer,  
Pedro Ruiz Fabian  
James Dawson

**May 25, 2016**

**University of Missouri  
Columbia, MO  
wasberg@missouri.edu**

## ACKNOWLEDGEMENT OF SPONSORSHIP

This research was funded by the Missouri (MO) Department of Transportation under project TR201605.

### **Disclaimer**

The opinions, findings and conclusions expressed in this publication are not necessarily those of the Departments of Transportation or the Federal Highway Administration. This report does not constitute a standard, specification or regulation.

## TABLE OF CONTENTS

List of Figures.....	i
List of Tables.....	iv
List of Appendices.....	iv
Executive Summary.....	1
1 Introduction.....	2
1.1 Background.....	2
2 Monitoring system.....	3
2.1 Accelerometers.....	3
2.2 Data Acquisition.....	4
2.3 Lab Testing.....	6
2.3.1 Required Data Acquisition Rates.....	7
2.4 Field Implementation Testing.....	9
2.5 Installation.....	11
3 Results.....	13
3.1 Estimated Event Rate.....	19
4 Conclusion.....	21
4.1 Recommendations.....	22
Appendix A.....	A-1
A.1 Node 48.....	A-1
A.2 Node 49.....	A-4
A.3 Node 50.....	A-7
A.4 Node 51.....	A-10

## LIST OF FIGURES

Figure 1. Elevation view of Bridge A-4497 showing the location of vertical members L21 and L21'.....	3
--	---

Figure 2: Image of a Microstrain G-Link sensor with its power supply and enclosure attached to the mounting plate. ....	4
Figure 3: Data acquisition system integrated with all the essential components. .	5
Figure 4: Sample data collection using the SensorConnect software.....	6
Figure 5: System lab setup. (A) data acquisition system attached to a column, (B) sensor node attached to a cabinet, (C) sensor node attach to a moving cart.....	7
Figure 6: Initial (left) and final (right) timing of the first oscillation at 10% of the original video speed. ....	8
Figure 7: Schematic of the placement of the data acquisition system and the wireless sensors (Google maps). ....	9
Figure 8: (A) Attachment of the data acquisition system, (B) attachment of sensor to a tension tie, (C) placement of sensor on the deck. ....	10
Figure 9: Types of impacts. (A) Impact on a tension tie via rubber mallet, (B) impact on the deck by jumping. ....	10
Figure 10: Data collected for Node 48.....	11
Figure 11: Installation of the data acquisition system. ....	12
Figure 12: Installation of one of the wireless sensor nodes.....	12
Figure 13. Schematic diagram showing location of sensor nodes mounted on verticals L21 and L21'. ....	13
Figure 14: Typical acceleration data from a vertical member showing two “events”. .....	14
Figure 15: Wind direction and degrees.....	18
Figure 16. Graph showing correlation between maximum winds and maximum accelerations. ....	19
Figure 17: Data collected for Node 48 between January 27, 2016 and February 1, 2016. ....	A-1
Figure 18: Data collected for Node 48 between February 1, 2016 and February 10, 2016. ....	A-2
Figure 19: Data collected for Node 48 between February 10, 2016 and February 15, 2016. ....	A-2

Figure 20: Data collected for Node 48 between February 29, 2016 and March 7, 2016.	A-3
Figure 21: Data collected for Node 48 between March 7, 2016 and March 14, 2016.	A-3
Figure 22: Data collected for Node 48 between March 14, 2016 and March 22, 2016.	A-4
Figure 23: Data collected for Node 49 between January 27, 2016 and February 1, 2016.	A-4
Figure 24: Data collected for Node 49 between February 1, 2016 and February 10, 2016.	A-5
Figure 25: Data collected for Node 49 between February 10, 2016 and February 15, 2016.	A-5
Figure 26: Data collected for Node 49 between February 29, 2016 and March 7, 2016.	A-6
Figure 27: Data collected for Node 49 between March 7, 2016 and March 14, 2016.	A-6
Figure 28: Data collected for Node 49 between March 14, 2016 and March 22, 2016.	A-7
Figure 29: Data collected for Node 50 between January 27, 2016 and February 1, 2016.	A-7
Figure 30: Data collected for Node 50 between February 1, 2016 and February 10, 2016.	A-8
Figure 31: Data collected for Node 50 between February 10, 2016 and February 15, 2016.	A-8
Figure 32: Data collected for Node 50 between February 29, 2016 and March 7, 2016.	A-9
Figure 33: Data collected for Node 50 between March 7, 2016 and March 14, 2016.	A-9
Figure 34: Data collected for Node 50 between March 14, 2016 and March 22, 2016.	A-10

Figure 35: Data collected for Node 51 between January 27, 2016 and February 1, 2016. ....	A-10
Figure 36: Data collected for Node 51 between February 1, 2016 and February 10, 2016. ....	A-11
Figure 37: Data collected for Node 51 between February 10, 2016 and February 15, 2016. ....	A-11
Figure 38: Data collected for Node 51 between February 29, 2016 and March 7, 2016. ....	A-12
Figure 39: Data collected for Node 51 between March 7, 2016 and March 14, 2016. ....	A-12
Figure 40: Data collected for Node 51 between March 14, 2016 and March 22, 2016. ....	A-13

## LIST OF TABLES

Table 1: A summary of the equipment installed on the Jefferson City Bridge and its location.....	13
Table 2: Occurrence times for the eleven “events” identified during the monitoring period. ....	15
Table 3: Node peak accelerations for each individual event.....	16
Table 4: Resonating frequency of the nodes for each event. ....	17
Table 5: Recorded wind speed and wind direction for each event. ....	18
Table 6: Average wind speed, standard deviation, and 95% confidence wind speed based on the events collected during field testing. ....	20
Table 7: Average wind direction, standard deviation, and 95% confidence wind direction based on the events collected during field testing.....	20

## LIST OF APPENDICES

Appendix A.....	A-1
-----------------	-----

## **EXECUTIVE SUMMARY**

The objective of the research was to determine the frequency and cause of resonant vibrations of truss verticals on bridge A4497 over the Missouri River in Jefferson City, MO. Instrumentation to monitor the vibrations of four verticals was installed on the bridge and monitored for 42 days. The instrumentation consisted of wireless accelerometers that monitored the accelerations on the four verticals. Weather data available from a weather station located at the Jefferson City Airport was used to analyze the weather conditions causing resonant vibrations of the verticals. It was found that there were eleven vibration “events” in which the vertical members vibrated with higher than normal accelerations. The average wind speed during the events was about 17 mph. The wind direction during the events was from the WNW/NW during nine of the events and from the SE for 2 of the events. It was found that the frequency of the events was 0.26 events per day during the monitoring period.

Historical weather data was analyzed to determine how frequently the resonance vibrations may be occurring, i.e., how frequently the combined wind speed and direction matched the conditions determined through the field monitoring. Historical weather data from 446 days was analyzed and it was found that there were 89 occurrences of the combined wind speed and direction that could cause vibrations of the vertical members. The resulting frequency of events was determined to be 0.20 events per day.

It was concluded that the frequency of resonant vibration events is likely 0.25 events per day or less. The vibrations are caused by average winds from the WNW/NW or SW of ~17 mph or greater, based on monitoring results. Recommendations stemming from the research were as follows:

1. The effect of the vibration events on the durability of the members should be analyzed further to determine if a retrofit is necessary. The data provided through the field monitoring should be used in the analysis.
2. Other vertical members of a similar length should be monitored to determine if they are affected by resonant vibrations.

# **1 INTRODUCTION**

This report documents research conducted to study resonant vibrations occurring on several vertical members of bridge A4497 crossing the Missouri River in Jefferson City, Missouri. Vibration of the vertical members was observed on several occasions by Missouri Department of Transportation (MoDOT) forces working in the area. The vibration of the vertical members was observed during periods of relatively high winds. It was not known how frequently the resonant vibrations were occurring. The actual wind speed and direction that excited resonance vibrations in the vertical members was not well defined.

The objective of the research was to determine the frequency and cause of resonant vibrations of truss verticals on bridge A4497 over the Missouri River in Jefferson City, MO. Instrumentation to monitor the vibrations of four verticals was installed on the bridge and monitored for 42 days. Weather data available from a weather station located at the Jefferson City Airport were used to analyze the weather conditions causing resonant vibrations of the verticals. Data were analyzed to determine how frequently resonance vibrations were occurring and to determine the ambient weather conditions of wind speed and direction that were causing the vibrations. Based on these data, historical weather data were analyzed to determine how frequently the resonance vibrations may be occurring, i.e., how frequently the combined wind speed and direction matched the conditions determined through the field monitoring.

## **1.1 Background**

Bridge A-4497 carries Rt. 54/63 across the Missouri River in Jefferson City, MO. The vertical members that were the subject of the study were members L21 and L21' as shown in Figure 1. There were four members monitored as part of the research; two on the East truss and two on the West truss. Member L21 is located on the west side of the truss centerline and L21' is located on the east side of the truss centerline. The I-shaped vertical members were comprised of two steel flanges (0.75 x 12 in.) and a web plate (0.375 x 19.5 in).

Instrumentation comprised of wireless accelerometers was installed on each of these vertical members to monitor vibrations. The following section of the report

describes the laboratory preparation work undertaken prior to installing the accelerometers on the bridge.

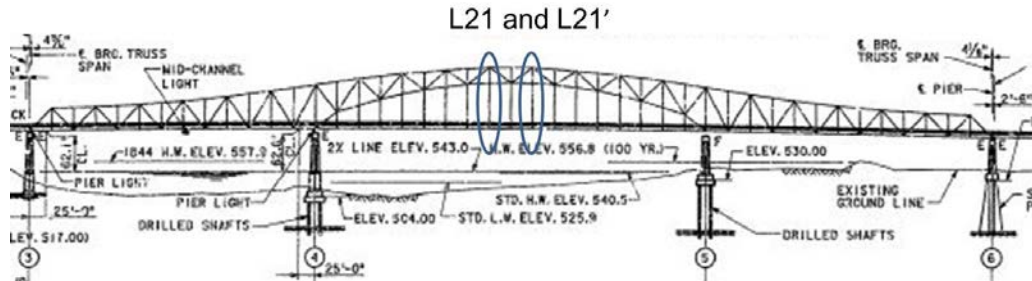


**Figure 1. Elevation view of Bridge A-4497 showing the location of vertical members L21 and L21'.**

## 2 MONITORING SYSTEM

This section of the report describes the field monitoring system that was developed to monitor the vibrations of the truss verticals. A hard-wired monitoring system in which each sensor was connected directly to a central data acquisition system was not practical because the vertical members that needed to be monitored were located on opposite sides of the truss. Therefore, wireless sensors were used to monitor the vibration of the vertical members.

### 2.1 Accelerometers

Four wireless Microstrain G-Link sensor nodes were used to monitor vibrations of the vertical members. The Microstrain G-Link sensor is a battery-operated high-speed tri-axial accelerometer with user-programmable sampling rates of up to 4096Hz. These sensors are capable of measuring accelerations of up to 10 g. Figure 2 shows a photograph of one of the sensor nodes. The sensor node and supporting batteries were mounted in a weather resistant enclosure. In order to attach the enclosure to the flanges of the vertical members, an aluminum mounting plate was fabricated and attached to the back of the enclosure. The mounting plate with the sensor enclosure was attached to the flanges of the vertical member using small flange clamps. In this orientation, the y-axis of the accelerometer was aligned vertically with the member such that vibrations resulting from member resonance would not be expected on the vertical axis of the sensor (channel

1). The x-axis and the z-axis of the accelerometer were aligned to detect flexural and torsional vibrations of the member. The four wireless sensor nodes are identified as Node 48, Node 49, Node 50, and Node 51.



**Figure 2: Image of a Microstrain G-Link sensor with its power supply and enclosure attached to the mounting plate.**

## 2.2 Data Acquisition

Figure 3 shows an image of the data acquisition system that is comprised of a Dell Laptop, Microstrain USB base station, Cisco router, and a conduit for power supply; these are all enclosed in a fiberglass enclosure. The data acquisition enclosure was used to protect the base station and computer from the elements. The laptop and USB base station were both attached to a mounting plate via screws and the mounting plate was attached to the fiberglass enclosure. The router was attached to the enclosure via Velcro strips. The laptop computer was used to run the software necessary for the wireless sensor nodes to communicate with the Microstrain USB base station and to store the data received from the sensors. The router was used for wireless communication with the computer for the purpose of downloading data. An Ethernet connection was also used to download the data. The system was powered by AC power provided on-site.



**Figure 3: Data acquisition system integrated with all the essential components.**

The software package, SensorConnect (beta version), was used for this research due to its ability to record and read the large data files collected during testing. Figure 4 is an image of the SensorConnect display screen with the USB base station and the nodes collecting data. The nodes were programmed to sample at a continuous rate of 16 Hz based on laboratory testing and video analysis as described in later sections of the report.

The SensorConnect software records data continuously and stores the data in computer memory. The data can then be retrieved through the attached router or Ethernet connection while the sensors continue to collect data. To post process the data, the downloaded files are inserted into the SensorConnect program on a separate computer. This file was manually analyzed to identify data of interest, i.e., periods where the vertical members were undergoing large amplitude vibrations. These data were exported for post-processing using the Microsoft Excel and Mathworks Matlab programs.



**Figure 4: Sample data collection using the SensorConnect software.**

### 2.3 Lab Testing

The monitoring system was tested in the laboratory to ensure proper operation of the monitoring systems. Testing in the lab was geared towards troubleshooting the data collection system and ensuring that data was being successfully collected and downloaded. Figure 5 illustrates the system in a lab setup. The data acquisition system was attached to a column to simulate the system attachment in the field and the sensor nodes were mounted to various objects in the lab, such as a cabinet or a moving cart. Data was collected over a time period of several weeks and downloaded periodically to simulate the anticipated field conditions. These tests were used to ensure that the software was operating reliably, data could be downloaded without interruption to the operation of the system, and so that estimates could be developed for the time required to download data sets of different sizes.

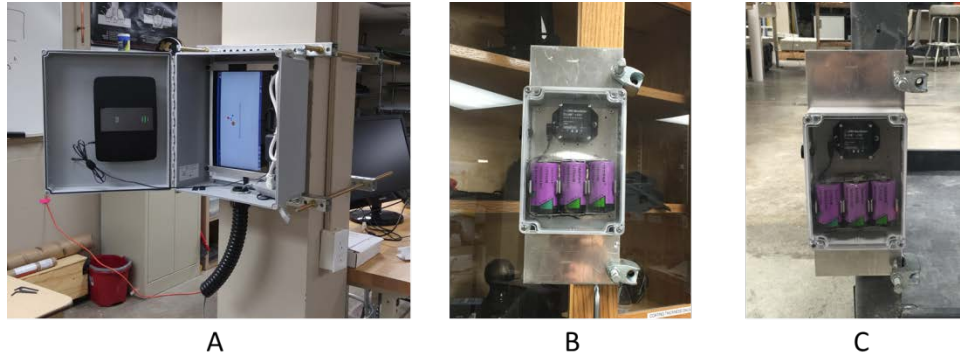


**Figure 5: System lab setup. (A) data acquisition system attached to a column, (B) sensor node attached to a cabinet, (C) sensor node attach to a moving cart.**

During the laboratory testing, it was found that the standard software provided with the system was inadequate for downloading datasets of the size required for field monitoring. Working with the manufacturer, a Beta version of an updated version of the software was acquired to support the field testing. This Beta version supported downloading and analyzing data sets of the size anticipated for the bridge monitoring project.

Based on the time required to download the data collected over time periods of several weeks, it was determined the wireless router was too slow to be practically implemented in the field. Therefore, a wired Ethernet connection was used for the field testing. The Ethernet connection was also successfully tested in the laboratory to collect and download data over time periods of several weeks.

### **2.3.1 Required Data Acquisition Rates**

Digital data acquisition of accelerometer data requires continuous, periodic, or threshold-based data collection. Periodic data collection is appropriate for health monitoring applications in which accelerations may vary over long time intervals. Monitoring the accelerations of a bridge for 1 hr each week in order to detect changes in acceleration that result from deterioration of bridge members is an example of periodic data collection. Threshold-based data collection means that data is only recorded to memory when defined threshold amplitudes of the acceleration are exceeded. Threshold-based data collection is appropriate when anticipated acceleration amplitudes are known either from previous experience or from analysis. For the JC Bridge, the anticipated acceleration amplitudes resulting from the vibration of the members were not known.

Consequently, continuous monitoring of the data was chosen as the approach for the research. Continuous monitoring of the acceleration data results in very large datasets that can be difficult to manage. Therefore, it was necessary to limit the data sampling rate to the greatest extent possible to limit the size of the resulting datasets. The data sampling rate is the number of data points stored to the computer memory per second. Generally, data sampling rates of at least twice the frequency of vibration are necessary to reproduce the frequency and amplitude of a signal that is captured digitally. To determine the minimum data sampling rate to be used to monitor vibrations of the JC Bridge, the video of a vertical member vibrating was analyzed.

The frequency of the vibration was determined by slowing down the video to 10% of its original speed using the software package Final Cut Pro™. The timing of a single oscillation was determined at the reduced speed and then converted back to the original video speed. Figure 6 shows the initial timing of the beginning of the oscillation and the final timing at the end of the oscillation. Note that the video is rotated 90 degrees. Once this time change was determined, the time was converted back to the original video time speed to calculate the frequency of vibration.

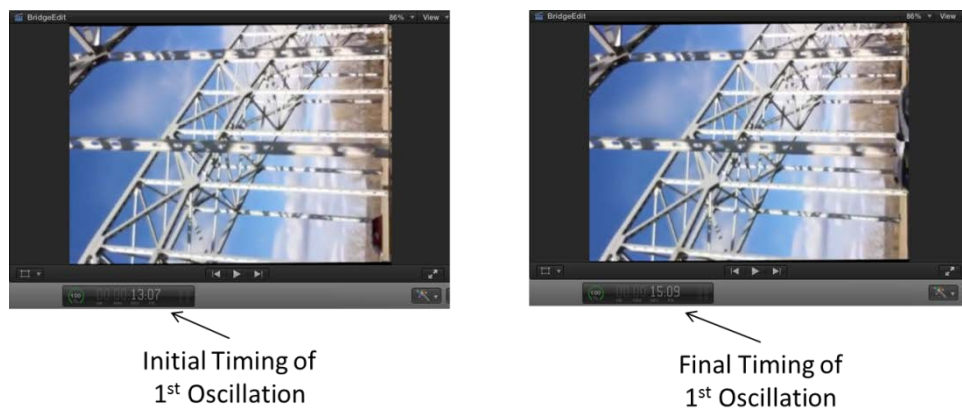


**Figure 6: Initial (left) and final (right) timing of the first oscillation at 10% of the original video speed.**

As shown in the figure, the change in time for a single oscillation was determined to be 0.203s. The frequency was then calculated to be 4.84Hz for a single cycle of vibration. A similar analysis was completed for five cycles of oscillations using the video at reduced speed. The time necessary for five oscillations was determined to be 9.90s. Based on these data, it was concluded that the members were oscillating at a frequency

of about 5 Hz. Therefore, a data sampling rate of at least 10 Hz would be necessary to capture the frequency content of the vibrations. Based on these data, a sampling rate of 16 Hz was used in the field. To ensure that this sampling rate would produce accurate results, data from a field implementation test were analyzed as described in the following section.

## 2.4 Field Implementation Testing

A field implementation test of the monitoring system was performed to ensure that all components of the system would perform adequately in the field and to practice field installation. The data acquisition system was installed on a vertical member of a pedestrian truss bridge located near the University of Missouri. During the test, nodes 48, 49, and 50 were attached to diagonal tension ties, and Node 51 was placed on the deck of the bridge. Figure 7 is a schematic of the placement of the data acquisition system and the wireless sensor nodes. The sensor nodes on the tension ties were mounted on tension ties that were observed to be carrying different amounts of tensile load based on their vibrations following an impact on the tie. Different amounts of tension in the diagonal ties produce different frequencies when impacted. This allowed for a variety of different vibration frequencies to be tested. Figure 8 shows the attachment of the data acquisition system to the vertical member and the sensor placement on the tension tie and the bridge deck.

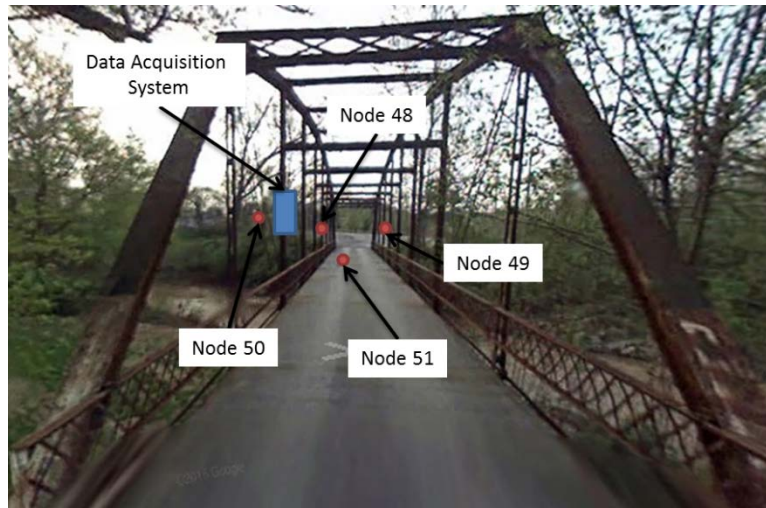


**Figure 7: Schematic of the placement of the data acquisition system and the wireless sensors (Google maps).**

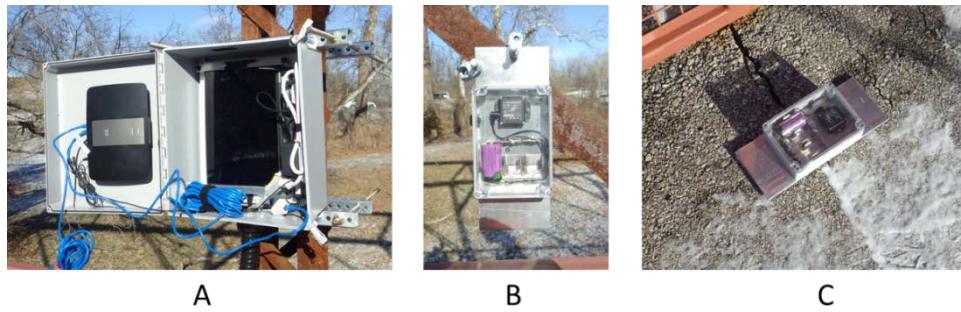


**Figure 8: (A) Attachment of the data acquisition system, (B) attachment of sensor to a tension tie, (C) placement of sensor on the deck.**

Testing of the sensors was completed by initiating the data acquisition software with a defined sampling rate of 4, 8, or 16 Hz. The diagonal tension tie was then impacted twice using a rubber hammer near each of the sensor nodes. The sensor node located on the bridge deck was excited by jumping on the bridge deck. Figure 9 shows the impacts on a tension tie with a rubber mallet (Figure 9A) and a jump near the sensor on the deck of the bridge (Figure 9B).



**Figure 9: Types of impacts. (A) Impact on a tension tie via rubber mallet, (B) impact on the deck by jumping.**

Figure 10 shows the results of the impacts near sensor Node 48 with different sampling rates used for each set of two impacts. The data shown in the figure was assembled from different tests (using different sampling rates) to illustrate the effect of different sampling rates. The effect of different data acquisition rates are clearly observed in the different impact sets. As shown in the figure, the amplitude of the impacts is not properly reproduced in the digital data when acquisition rates of less than 16 Hz were used. This effect is caused by the under sampling of data, i.e., data sampling rate not

being sufficiently high. Sampling rates of greater than 16 Hz were not considered due to practical limitations. Specifically, data sets would be too large to be efficiently downloaded in the field. Because the sampling rate of 16 Hz was three times the frequency calculated through the video analysis and exceeds the minimum sampling rate of 10 Hz, it was determined to be adequate to meet the objectives of the research. Using the sampling rate of 16 Hz, seven days of data collection from the four accelerometers produced two Gigabytes of data.

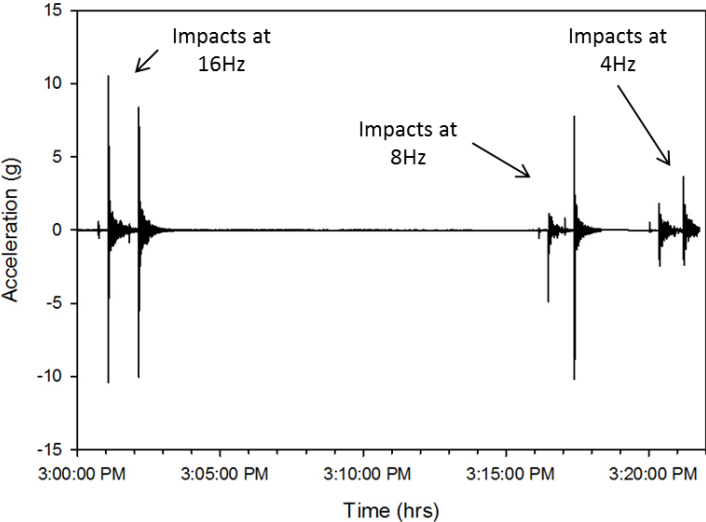


**Figure 10: Data collected for Node 48.**

### 2.5 Installation

The installation of the field monitoring system was completed with the aid of MoDOT on Wednesday, January 27, 2016. Installation began by closing down the right driving lane of the bridge to allow for the installation of AC power necessary for the monitoring system to operate. Once the power was installed, the data acquisition system was installed about 10 feet up on vertical member L22 on the east side of the bridge. Figure 11 shows the data acquisition system installed on the vertical member. After the installation of the data acquisition system, the system was tested and data was downloaded to ensure that all sensor nodes were working properly and communicating with the base station. Installation of two of the wireless sensors, Node 48 and Node 49, followed. Node 48 was installed on vertical member L21 on the southeast side of the bridge, while Node 49 was installed on vertical member L21' on the northeast side of the

bridge. Node 50 was installed on vertical member L21' on the northwest side of the bridge, while Node 51 was installed on vertical member L21 on the southwest side of the bridge. Figure 12 is a photograph of one of the wireless sensor nodes being installed. All four of the wireless sensors were installed approximately 30 feet above the roadway.



**Figure 11: Installation of the data acquisition system.**



**Figure 12: Installation of one of the wireless sensor nodes.**

Table 1 includes a summary of the location of the sensor nodes as mounted on the JC Bridge. Figure 13 shows the locations of the sensor nodes on the JC Bridge in a schematic diagram. In the figure, the elevation view of the bridge is shown (top) and the location of the sensor nodes on the verticals is shown.

**Table 1: A summary of the equipment installed on the Jefferson City Bridge and its location.**

Equipment	Member	Location
Data Acquisition System	L22	east side
Node 48	L21	southeast side
Node 49	L21'	northeast side
Node 50	L21'	northwest side
Node 51	L21	southwest side

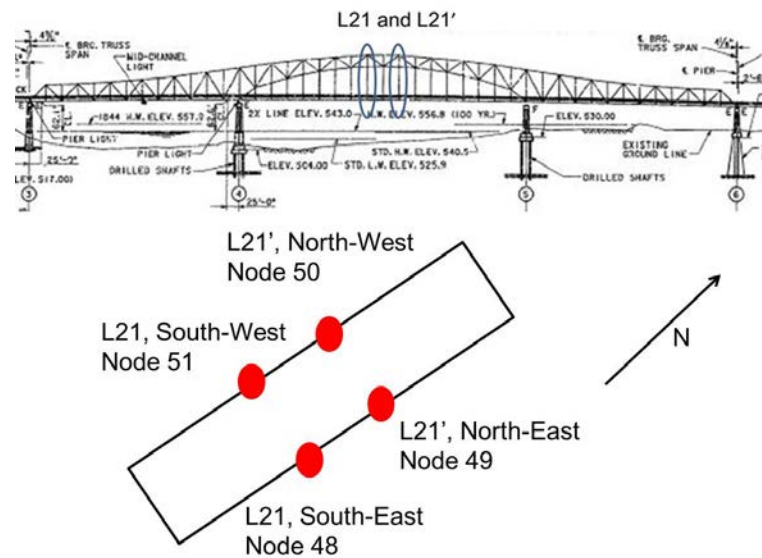


**Figure 13. Schematic diagram showing location of sensor nodes mounted on verticals L21 and L21'.**

### 3 RESULTS

Testing of the Jefferson City Bridge began on January 27, 2016, and was continued until February 15, 2016. At that time, testing stopped due to a loss of communication between the wireless sensor nodes and the data acquisition system. The cause of this loss of communication was not known and could not be reproduced in the laboratory. The computer used for data acquisition was replaced in an effort to eliminate the cause of the loss of communication. The system was restarted on February 29, 2016 and data was collected until the system was removed on March 22, 2016. The system was removed at that time for two reasons. First, the monitoring system indicated that

communication with the sensor nodes had been lost. It was later realized that communication had not been lost, and data was still being collected even though the system indicated it was not being collected. Regardless, the system needed to be removed prior to the start of a maintenance project that would limit the ability to support lane closures necessary on the bridge. In total, data were collected for 42 days.

Data collected during this time period was analyzed to identify when resonance vibrations were occurring on the bridge. The nominal vibrations occurring on the verticals during normal traffic loading was analyzed and it was determined that the nominal vibrations were generally 0.25 g or less. Based on these data, a resonance “event” was identified as a vibration amplitude of greater than 0.25 g for an extended period of time, typically more than 1 hr. Figure 14 shows typical data collected on a vertical member. As shown in the figure, events were identified from the peak amplitudes of vibrations. During the 42 days of testing, eleven different “events” were identified in the data. As shown in Figure 14, vibration amplitudes varied during a typical “event” and these variations were grouped together to form an individual “event.”

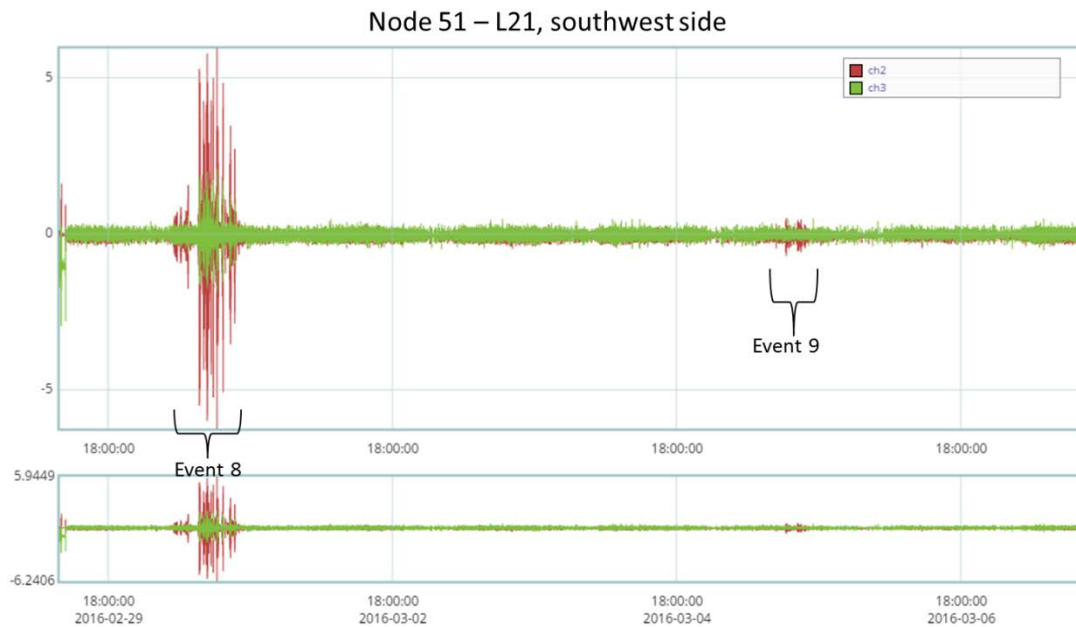


**Figure 14: Typical acceleration data from a vertical member showing two “events”.**

Table 2 shows all eleven events that occurred during the monitoring period along with their time of occurrence and the duration of the event. As shown in the table, the “events” typically occurred during the daytime, between the hours of 5:00 am and 9:00

pm. One of the events lasted for several days. The duration of the events ranged from a low of 1.5 hrs to a maximum of 45 hrs. As noted previously, the amplitudes of the vibrations varied during the course of an event, such that the high-amplitude vibrations were not continuous throughout the 45 hr time period. All of the different events identified during the monitoring are shown in Appendix A.

**Table 2: Occurrence times for the eleven “events” identified during the monitoring period.**

Event	Start Date	End Date	Start Time	End Time	Duration (hrs)
#1	1/28/2016	1/28/2016	1:00pm	5:30pm	4.5
#2	1/31/2016	1/31/2016	12:30pm	2:00pm	1.5
#3	2/2/2016	2/2/2016	5:30am	8:00am	2.0
#4	2/3/2016	2/3/2016	10:00am	2:30pm	4.5
#5	2/7/2016	2/9/2016	10:00pm	7:00pm	45.0
#6	2/12/2016	2/12/2016	11:00am	3:00pm	4.0
#7	2/13/2016	2/14/2016	11:30pm	6:30am	7.0
#8	3/1/2016	3/1/2016	5:00am	4:30pm	11.5
#9	3/5/2016	3/5/2016	12:00pm	4:00pm	4.0
#10	3/15/2016	3/15/2016	5:00pm	9:00pm	4.0
#11	3/19/2016	3/19/2016	11:00am	2:00pm	3.0

As shown in Figure 14, data was collected only for channels two and three of the tri-axial node sensors. Channel 2 and channel 3 collected data in the x-axis and z-axis respectively as described previously. The peak acceleration for channels 2 and 3 of each individual node for each event is shown in Table 3. These peak accelerations were determined by finding the highest acceleration experienced during an individual event. The greatest peak lateral accelerations occurred on Node 51 (L21, southwest) with an acceleration of 7.10g, while the greatest peak torsional acceleration also occurred in the same node with an acceleration of 2.44g. Overall, Node 51 exhibited the highest peak acceleration, both laterally and torsional for all of the events analyzed. The second highest overall peak lateral acceleration occurred in Node 50 (L21', northwest), while the second highest overall peak torsional acceleration occurred in Node 48 (L21, southeast).

**Table 3: Node peak accelerations for each individual event.**

Event	Peak Acceleration (g)							
	Node 48		Node 49		Node 50		Node 51	
	Chan. 2	Chan. 3	Chan. 2	Chan. 3	Chan. 2	Chan. 3	Chan. 2	Chan. 3
#1	0.45	0.3	0.46	0.24	0.52	0.29	0.56	0.36
#2	0.49	0.29	0.44	0.16	0.31	0.28	0.39	0.27
#3	1.42	0.35	1.23	0.29	0.44	0.27	1.28	0.48
#4	1.84	0.69	1.70	0.63	3.09	1.13	5.82	1.96
#5	2.93	1.05	1.92	0.69	4.20	1.46	7.10	2.44
#6	0.62	0.33	0.54	0.26	0.99	0.39	3.20	1.09
#7	1.75	0.70	0.70	0.26	0.82	0.35	3.73	1.38
#8	2.03	1.15	1.34	0.52	2.45	0.96	5.94	2.08
#9	0.43	1.00	0.46	0.17	0.48	0.27	0.52	0.46
#10	0.66	0.96	0.66	0.23	0.59	0.31	0.83	0.42
#11	0.68	0.52	0.53	0.17	0.44	0.19	0.95	0.37
Ave.	1.21	0.67	0.91	0.33	1.30	0.54	2.76	1.03

A frequency analysis was also conducted on the data collected for each event. The purpose of the frequency analysis was to determine the frequency at which the verticals were resonating and to confirm the video analysis. The data for each individual event was analyzed with a Fast Fourier Transform (FFT) using a MatLab program. The results of this analysis determined the frequency of the resonating verticals. Table 4 details the frequency that each node was resonating during each event. The highest frequency of 5.32Hz occurred on Node 48 and the slowest frequency of 5.21Hz occurred on Node 50. From the table, the average overall frequency was of 5.27Hz. The average frequency is 8.8% higher than the original calculated frequency of 4.84Hz from the video analysis. Generally, there was little variation in the vibration frequencies determined for the different verticals and for the different events.

**Table 4: Resonating frequency of the nodes for each event.**

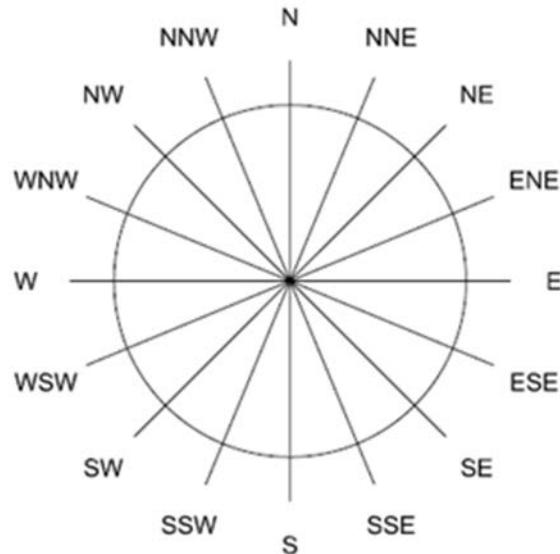
Event	Frequency (Hz)							
	Node 48		Node 49		Node 50		Node 51	
	Chan. 2	Chan. 3	Chan. 2	Chan. 3	Chan. 2	Chan. 3	Chan. 2	Chan. 3
#1	5.32	5.32	5.30	5.30	5.23	5.23	5.24	5.23
#2	5.31	5.31	5.28	5.28	5.23	5.23	5.23	5.23
#3	5.32	5.32	5.30	5.30	5.24	5.24	5.24	5.24
#4	5.31	5.31	5.29	5.29	5.22	5.22	5.23	5.23
#5	5.31	5.31	5.29	5.29	5.22	5.22	5.23	5.23
#6	5.32	5.32	5.30	5.30	5.23	5.23	5.23	5.23
#7	5.32	5.32	5.30	5.30	5.24	5.24	5.24	5.24
#8	5.30	5.30	5.29	5.29	5.22	5.22	5.23	5.23
#9	5.31	5.31	5.29	5.29	5.23	5.23	5.24	5.24
#10	5.30	5.30	5.28	5.28	5.21	5.21	5.22	5.22
#11	5.31	5.31	5.29	5.29	5.23	5.23	5.23	5.23
Ave.	5.31	5.31	5.29	5.29	5.23	5.23	5.23	5.23

Table 5 details the wind speed and wind direction for each event that occurred during field testing. The average wind speed and wind direction reported in the table is an average of the conditions during the duration of the event. The high and low values during the event are also shown. The wind conditions were tracked using the wind readings at the nearest weather station located at the Jefferson City Memorial Airport. The data was tracked online at [weatherunderground.com](http://weatherunderground.com). Wind speeds reported by the weather service are based on a two minute wind speed average. In every hour, a two minute time period is selected in which wind speed measurements are recorded every five seconds. The average of these measurements is then called the wind speed for that hour. The lowest average wind velocity that was observed during an event was of 14.3 mph, while the highest average wind velocity observed was of 23.7 mph. The wind directions are recorded in degrees. Figure 15 illustrates the correlation between the wind directions in degrees with its cardinal direction counterpart. From Table 5, two events occurred with average wind directions ranging between 115.0° to 123.3°, i.e., with winds coming out of the ESE. The remaining nine events had an average wind direction ranging from 290.0° to 310.0°, i.e., with winds coming out of the WNW and NW.

**Table 5: Recorded wind speed and wind direction for each event.**

Event	Wind Speed (mph)			Wind Direction (deg)		
	Low	High	Average	Low	High	Average
#1	15.0	20.7	17.3	300.0	320.0	308.0
#2	13.8	20.7	17.3	300.0	310.0	305.0
#3	16.1	21.9	19.0	110.0	120.0	115.0
#4	13.8	23.0	18.6	280.0	310.0	294.3
#5	11.5	29.9	17.4	280.0	320.0	306.0
#6	11.5	19.6	15.5	290.0	350.0	307.1
#7	12.7	18.4	15.1	110.0	140.0	123.3
#8	6.9	24.2	16.9	260.0	320.0	301.3
#9	10.4	17.3	14.3	300.0	320.0	310.0
#10	15.0	31.1	23.7	270.0	300.0	290.0
#11	12.7	18.4	15.6	280.0	320.0	300.0

Cardinal Direction	Degree Direction
N	348.75 - 11.25
NNE	11.25 - 33.75
NE	33.75 - 56.25
ENE	56.25 - 78.75
ESE	78.75 - 101.25
ESE	101.25 - 123.75
SE	123.75 - 146.25
SSE	146.25 - 168.75
S	168.75 - 191.25
SSW	191.25 - 213.75
SW	213.75 - 236.25
WSW	236.25 - 258.75
W	258.75 - 281.25
WNW	281.25 - 303.75
NW	303.75 - 326.25
NNW	326.25 - 348.75



**Figure 15: Wind direction and degrees.**

Figure 16 shows the correlation between the maximum winds recorded for each event with the maximum acceleration measured by each sensor node. As shown in the figure, sensor node 51 typically exhibited much higher accelerations than other sensor nodes; sensor node 50 also exhibited higher accelerations than other sensor nodes. These sensor nodes were located on verticals L21 and L21' on the west side of the bridge.

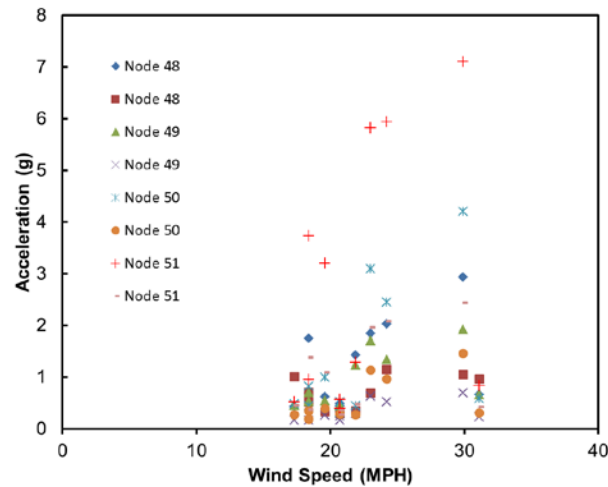


**Figure 16. Graph showing correlation between maximum winds and maximum accelerations.**

### 3.1 Estimated Event Rate

The field monitoring and data analysis described above provided the characteristic wind speed and direction that caused resonant vibrations in the vertical members. The monitoring provided a limited sampling period of 42 days during which 11 events occurred. To extend the analysis and determine how frequently the events were occurring over the course of a year or more, historical weather data from the Jefferson City Airport was analyzed. These data were analyzed statistically to determine the rate at which the events may be occurring.

The average wind speed for the winds coming out of the northwest and southeast are shown in Table 6. The average wind speed for winds out of the WNW/NW is 17.4 mph with a standard deviation ( $\sigma$ ) of 2.7 mph, while the average wind speed for the winds out of the SE was 17.0 mph with a standard deviation of 2.8 mph. From Table 7, the average wind direction for the nine events coming out of the WNW/NW was of  $302.4^\circ$  with a standard deviation of  $6.7^\circ$ , while the average wind direction for the two events out of SE being  $119.2$  with a standard deviation of  $5.9^\circ$ .

The average and standard deviation were used for a wind speed and wind direction analysis of historical data. Weather data was obtained for 446 days starting January 1, 2015 through March 21, 2016. These data were analyzed in Excel using the averages

obtained from the event recorded during field monitoring. It was assumed that these data were normally distributed such that using +/- two standard deviations ( $\sigma$ ) would capture all events with a confidence that exceeded 95%. The values for this can be seen in Table 6 and Table 7 for the wind speed and wind direction respectively. For the wind speed, only the  $-2\sigma$  was used since this was a minimum threshold.

Historical weather data was analyzed by determining the number of hours in which the combined wind speed and direction occurred during the 446 days. This number of hours was then divided by the average time period for events as determined from the field testing.

Using these parameters and the average duration of the events for both winds coming out of the WNW/NW and SE, it was determined that 56 events would have come out of the WNW/NW, while 33 events would have been from the SE. That is a total of 89 events exhibiting the weather conditions that result in resonance phenomenon during the 446 day time period that weather data was analyzed. This is a rate of 0.20 events/day, or one event every 5 days. From the field monitoring, 11 events were recorded in 42 days for a rate of 0.26 events per day, or about one event every four days. The return rates determined from the field monitoring and from analysis of historical weather data were of a similar order of magnitude.

**Table 6: Average wind speed, standard deviation, and 95% confidence wind speed based on the events collected during field testing.**

	Wind Speed (mph)	
	WNW/NW	SE
Average	17.4	17.0
$\sigma$	2.7	2.8
$-2\sigma$	12.0	11.5

**Table 7: Average wind direction, standard deviation, and 95% confidence wind direction based on the events collected during field testing.**

	Wind Direction (deg)	
	WNW/NW	SE
Average	302.4	119.2
$\sigma$	6.7	5.9
$-2\sigma$	289	107
$2\sigma$	316	131

## 4 CONCLUSION

The objective of the research was to determine the frequency and cause of resonant vibrations of truss verticals on bridge A4497 over the Missouri River in Jefferson City, Missouri. Data from field monitoring was used to identify when resonant vibrations were occurring and to identify the wind speed and direction at the time of the vibrations. Historical weather data was also analyzed to determine how frequently the defined wind speed and direction combination occurred over a time interval of 446. From these data, the rate of occurrence of the resonant vibrations was determined.

It was concluded that the frequency of resonant vibration events is likely 0.25 events per day or less. The vibrations are caused by average winds from the WNW/NW or SW of ~17 mph or greater, based on monitoring results. The specific conclusions from the monitoring and analysis of historical weather data were as follows:

- Field monitoring data analysis
  - 42 days of data were collected with eleven events occurring at a rate of 0.26 events/day during the field testing time period
  - The average wind direction for nine of the events was from the WNW/NW and for the remaining two events from the SE
  - Average wind speeds from the WNW/NW winds was of 17.4 mph ranging from 14.3 mph to 23.7 mph
  - Average wind speeds from the SE winds was of 17.0 mph ranging from 15.1 mph to 19.0 mph
  - Lowest maximum wind speed to result in an event was 17.3 mph
- Historical weather data analysis
  - 446 days of data were collected with 89 events occurring at a rate of 0.20 events/day during the time period data was analyzed
  - 56 of the events with winds from the WNW/NW were found with the remaining 33 events with winds from the SE
  - A difference of only 0.06 events/day or 23.1% was observed between the data collected during field testing

## 4.1 Recommendations

The research to date determined the characteristic weather conditions and frequency of resonant vibrations of four vertical members on the JC Bridge. The research did not attempt to analyze the effect of these vibrations on the durability of the bridge members. The research led to the following recommendations

1. The effect of the vibration events on the durability of the members should be analyzed further to determine if a retrofit is necessary. The data provided through the field monitoring should be used in the analysis. Additional monitoring should be considered if a retrofit is installed.
2. Other vertical members of a similar length should be monitored to determine if they are affected by resonant vibrations. The members that were monitored were selected based on previous observed vibrations; other member may be similarly affected, perhaps with lower magnitude vibrations that are not easily observed visually.

## APPENDIX A

The following appendix provides all of the data that was collected by the accelerometers during the field testing time period. The data is organized per node installed on the bridge members. For the location of each node, Table 1 can be referenced.

### A.1 Node 48

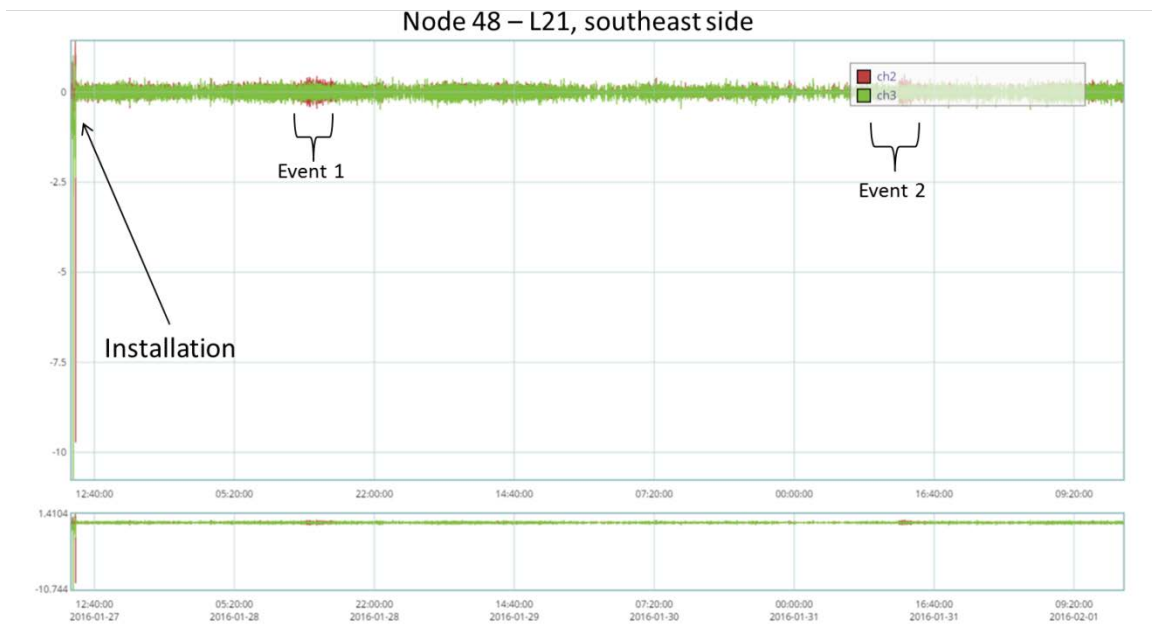


Figure 17: Data collected for Node 48 between January 27, 2016 and February 1, 2016.

Node 48 – L21, southeast side

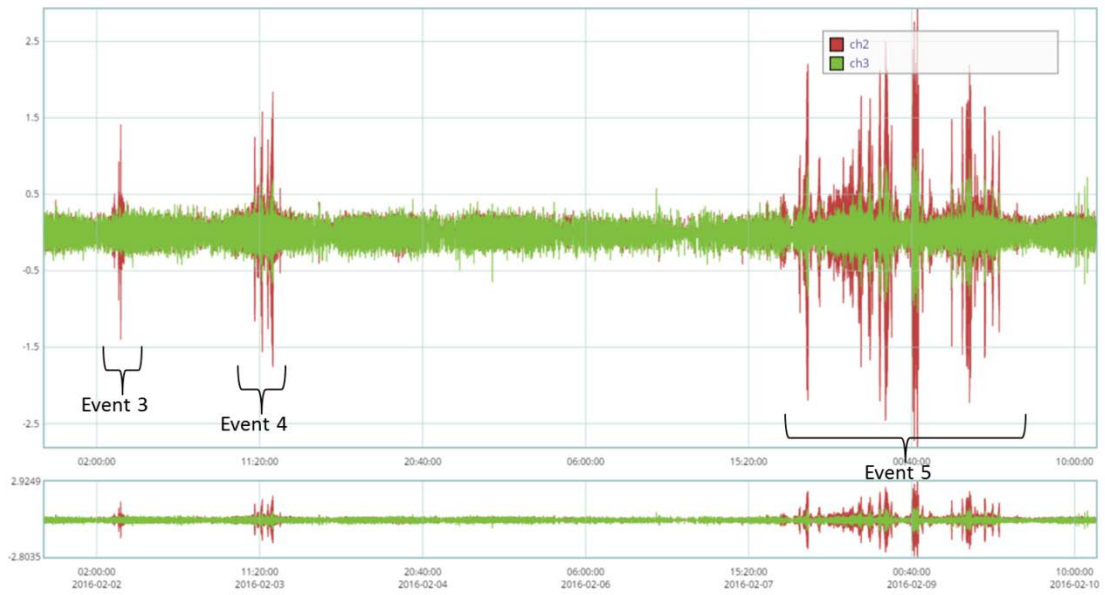


Figure 18: Data collected for Node 48 between February 1, 2016 and February 10, 2016.

Node 48 – L21, southeast side

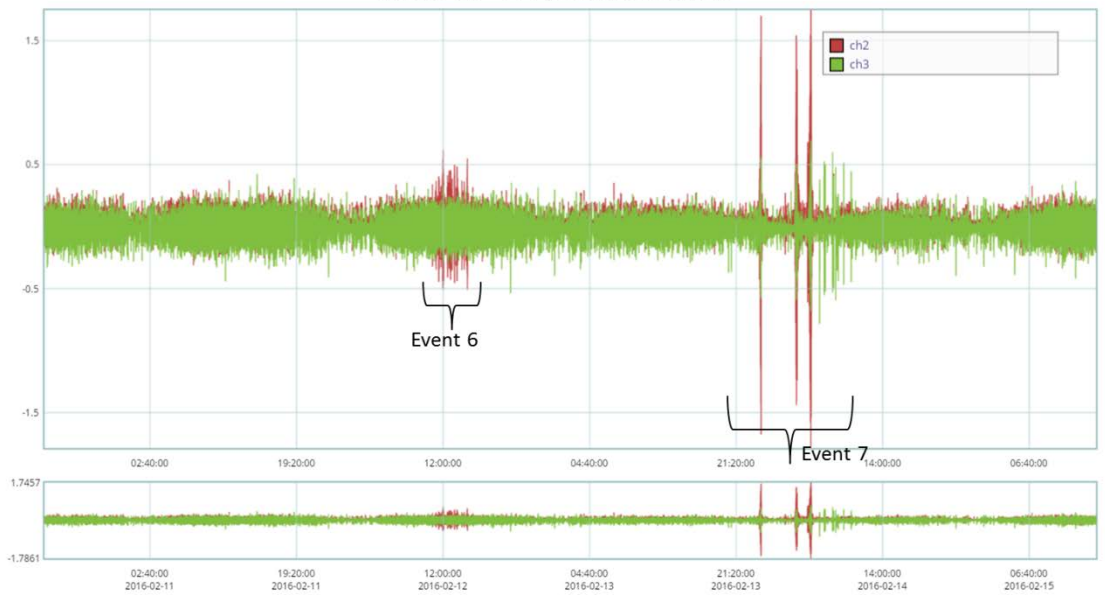
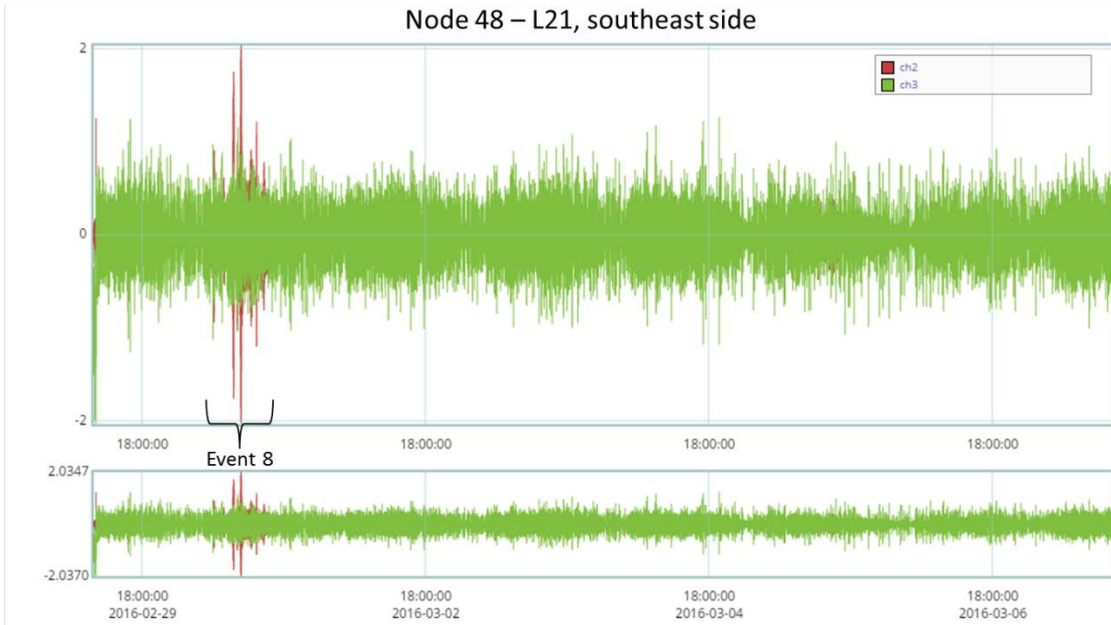
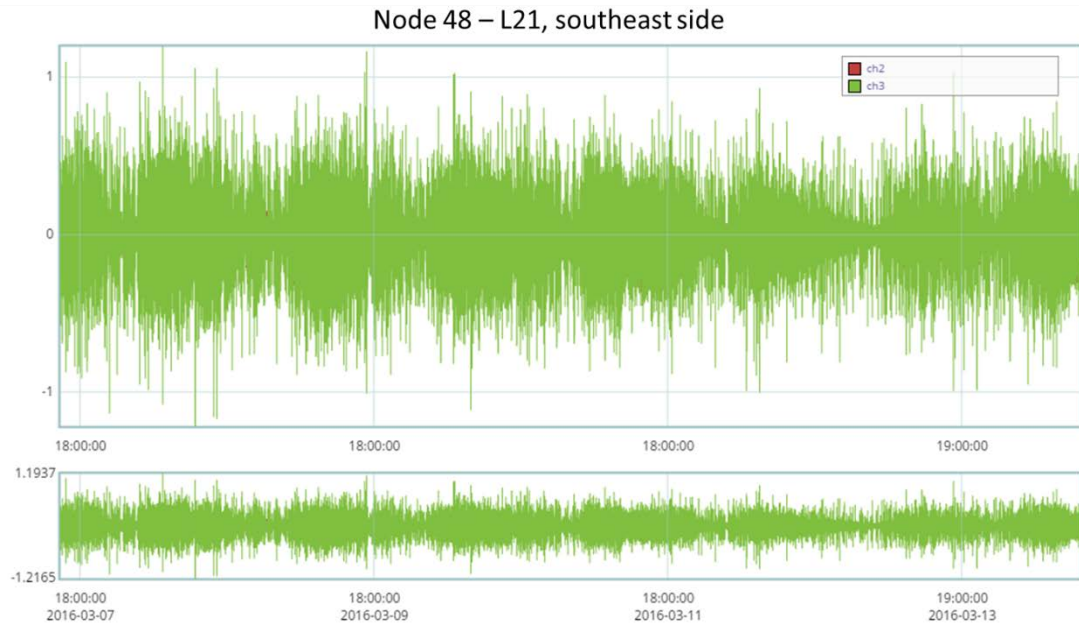


Figure 19: Data collected for Node 48 between February 10, 2016 and February 15, 2016.



**Figure 20: Data collected for Node 48 between February 29, 2016 and March 7, 2016.**



**Figure 21: Data collected for Node 48 between March 7, 2016 and March 14, 2016.**

Node 48 – L21, southeast side

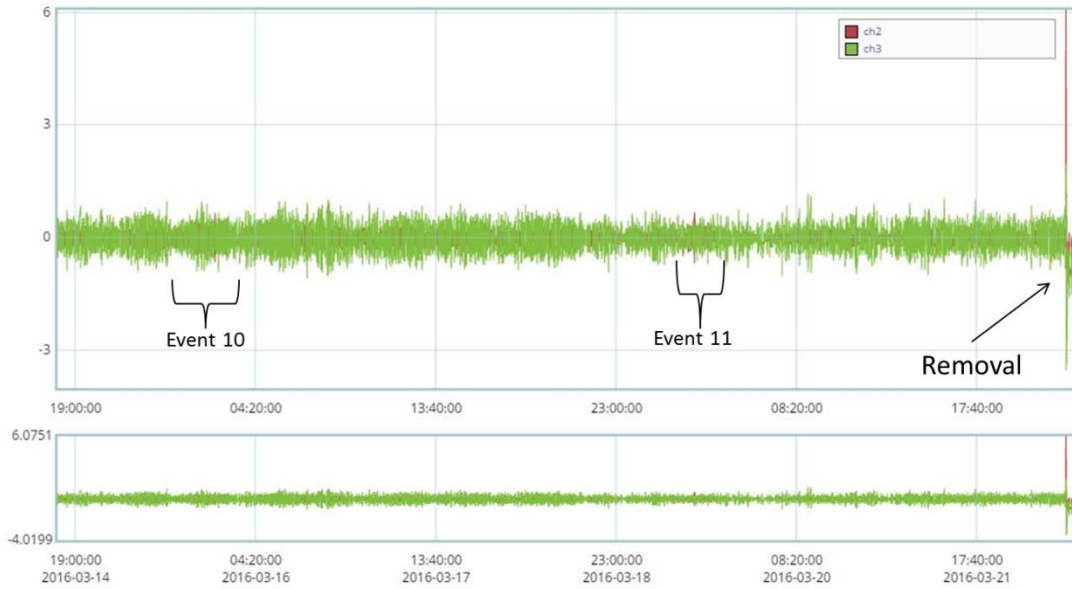


Figure 22: Data collected for Node 48 between March 14, 2016 and March 22, 2016.

## A.2 Node 49

Node 49 – L21', northeast side

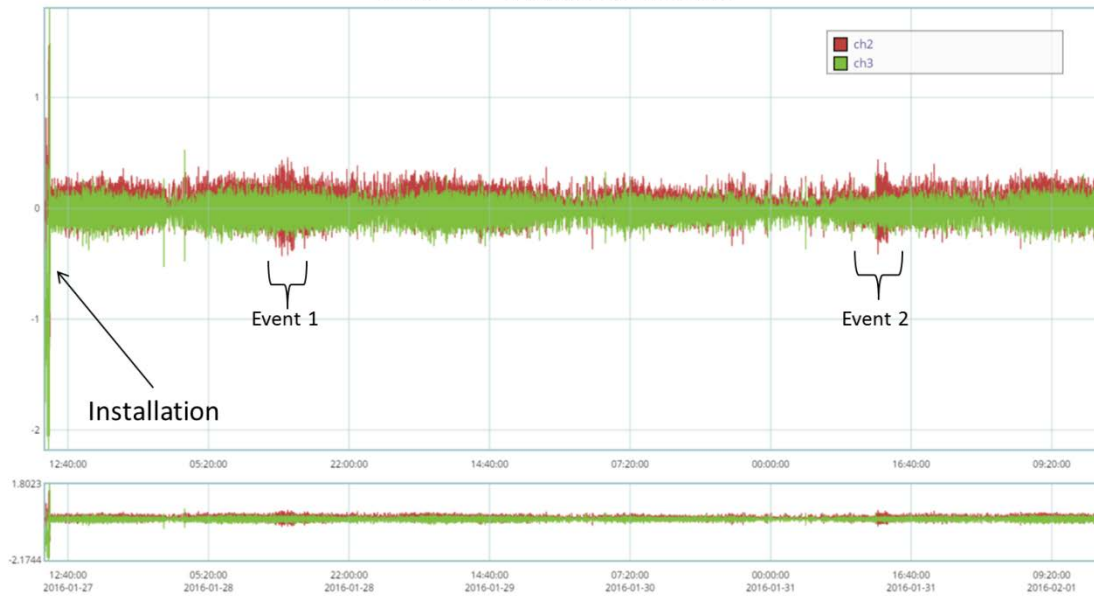


Figure 23: Data collected for Node 49 between January 27, 2016 and February 1, 2016.

Node 49 – L21', northeast side



Figure 24: Data collected for Node 49 between February 1, 2016 and February 10, 2016.

Node 49 – L21', northeast side

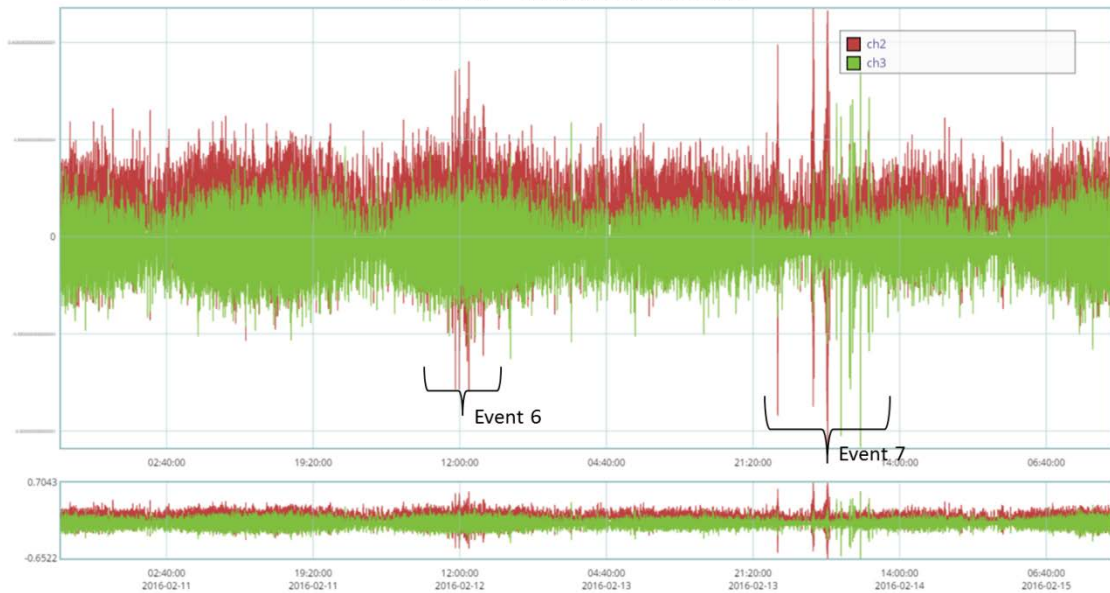
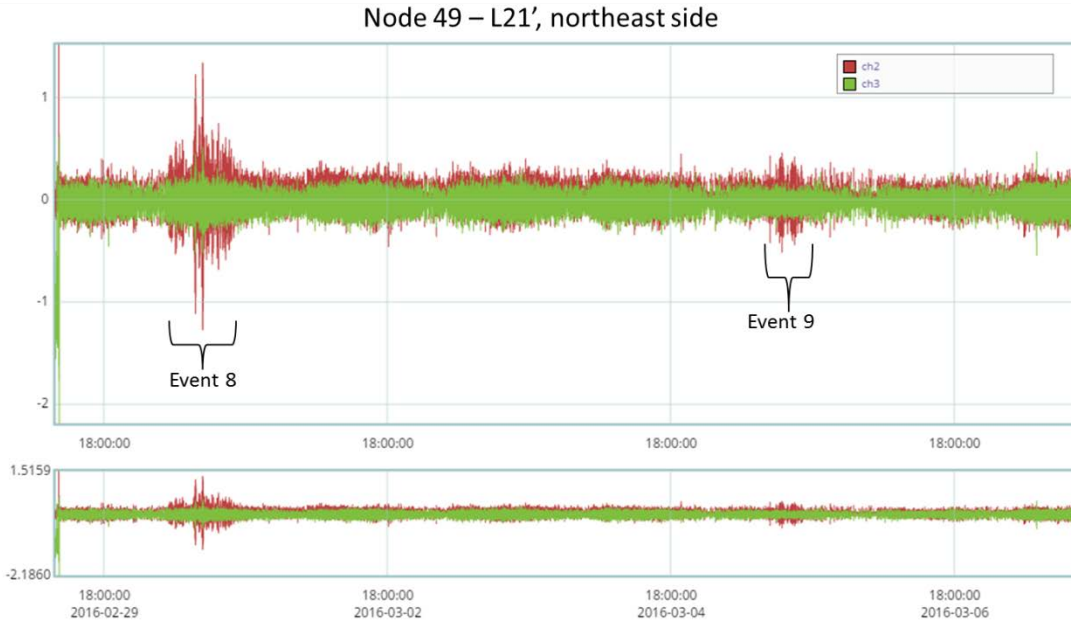
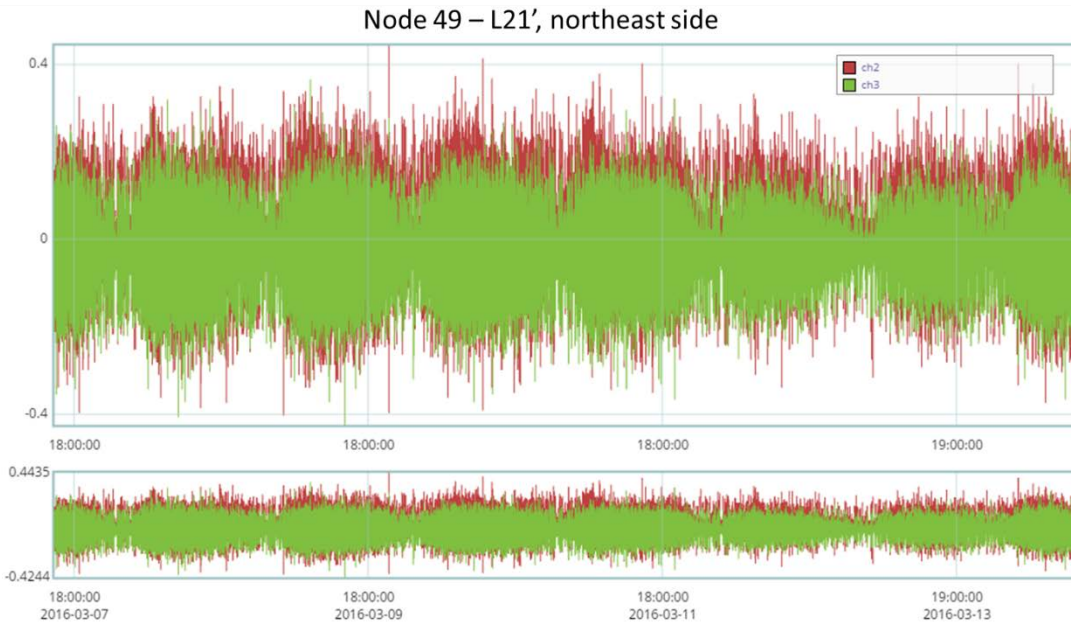


Figure 25: Data collected for Node 49 between February 10, 2016 and February 15, 2016.



**Figure 26: Data collected for Node 49 between February 29, 2016 and March 7, 2016.**



**Figure 27: Data collected for Node 49 between March 7, 2016 and March 14, 2016.**

Node 49 – L21', northeast side

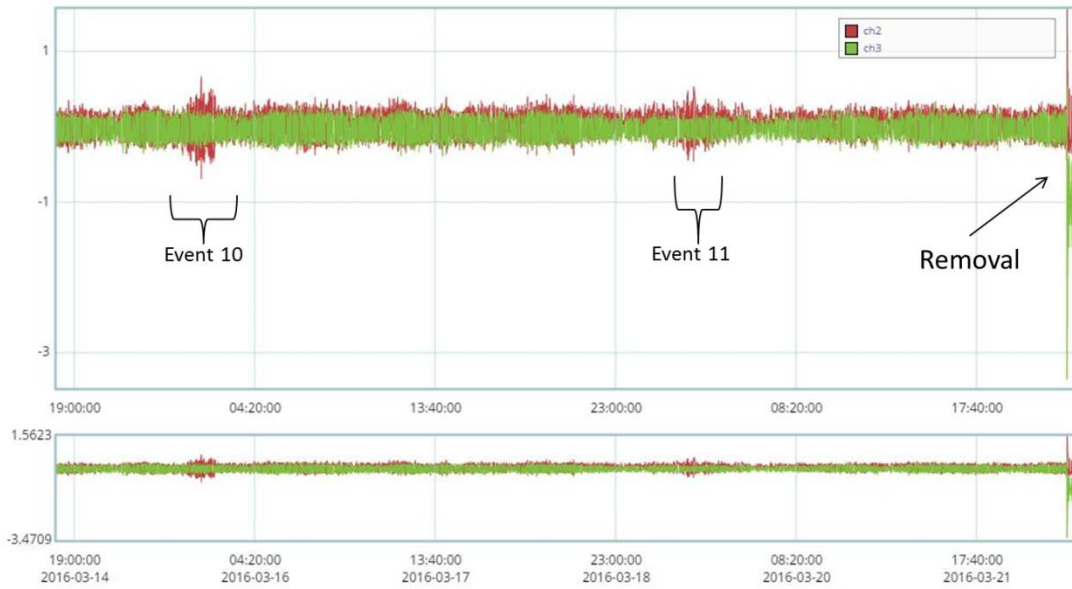


Figure 28: Data collected for Node 49 between March 14, 2016 and March 22, 2016.

### A.3 Node 50

Node 50 – L21', northwest side

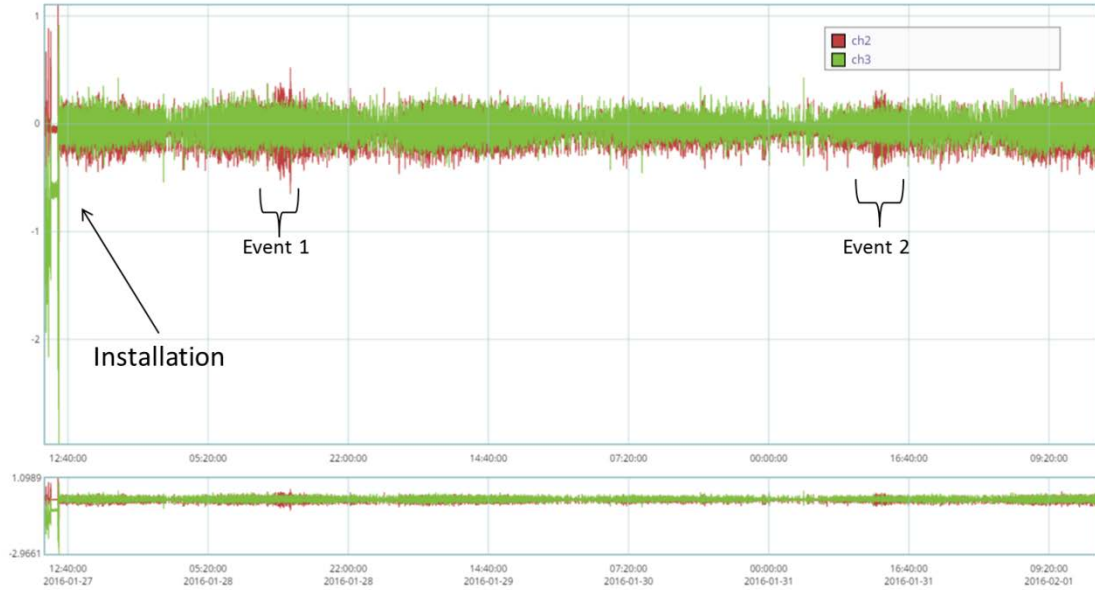


Figure 29: Data collected for Node 50 between January 27, 2016 and February 1, 2016.

Node 50 – L21', northwest side

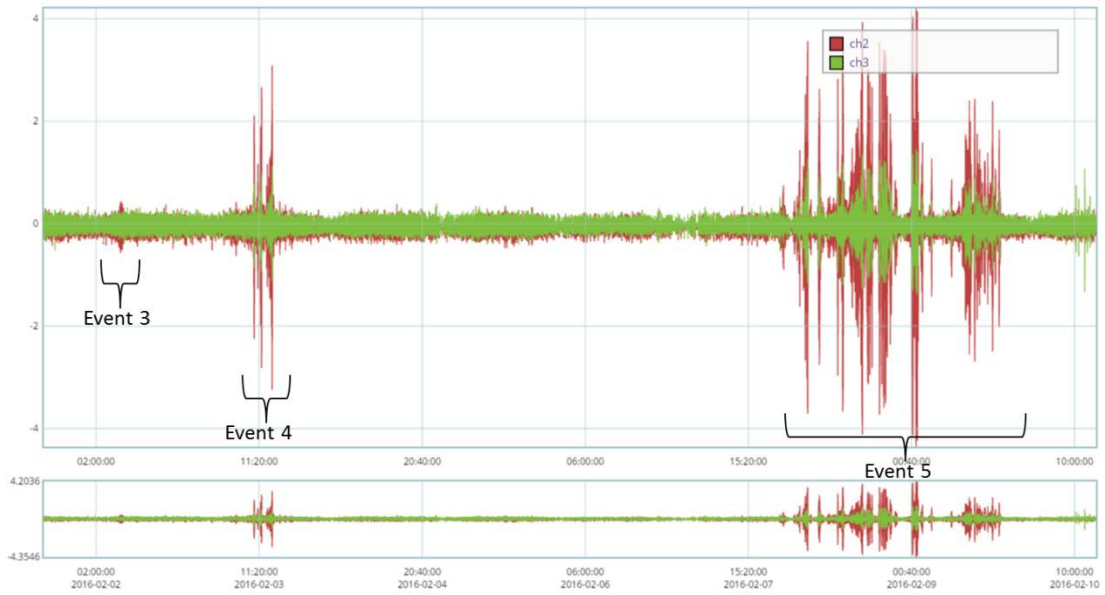


Figure 30: Data collected for Node 50 between February 1, 2016 and February 10, 2016.

Node 50 – L21', northwest side

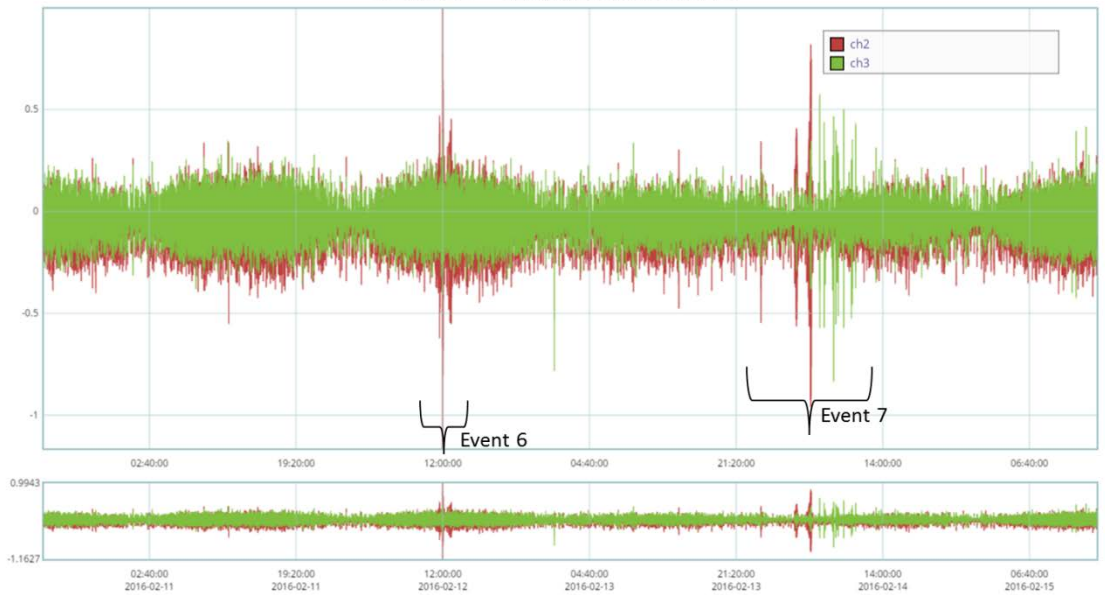
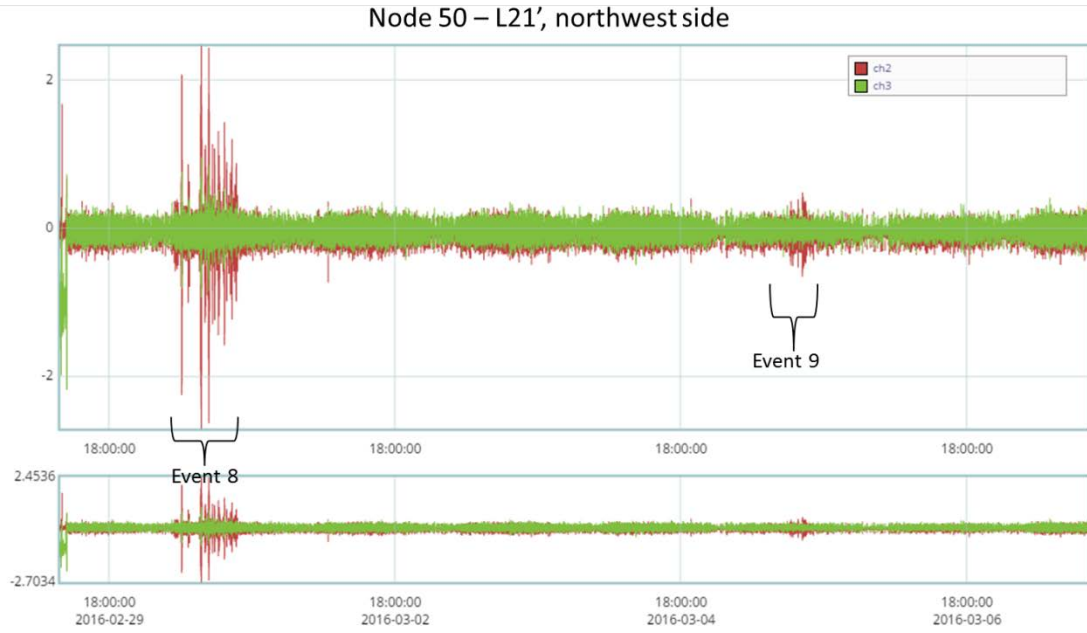
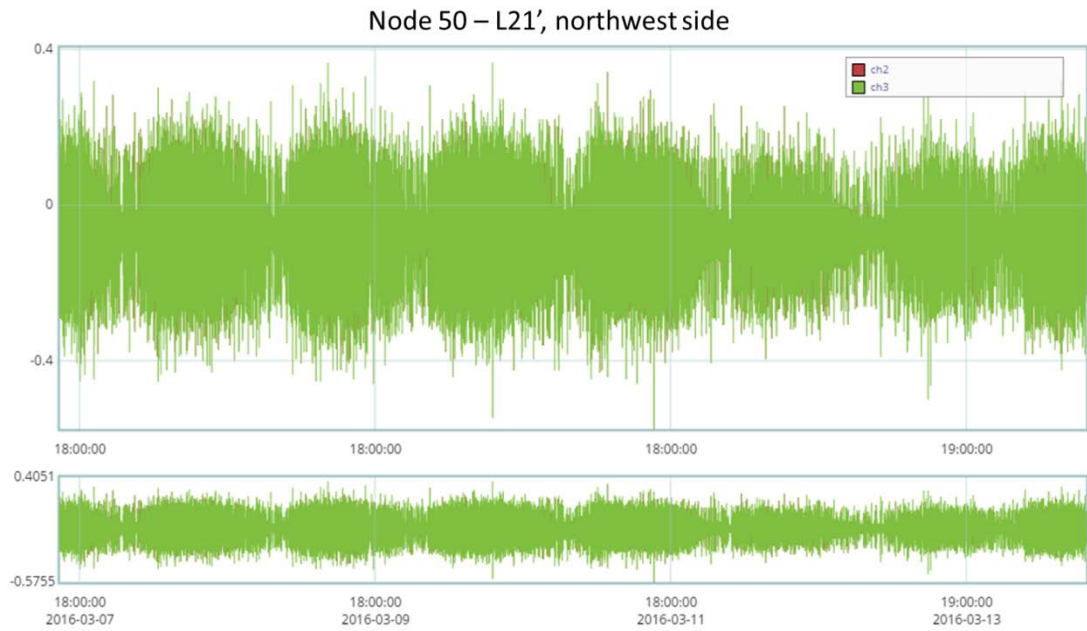


Figure 31: Data collected for Node 50 between February 10, 2016 and February 15, 2016.



**Figure 32: Data collected for Node 50 between February 29, 2016 and March 7, 2016.**



**Figure 33: Data collected for Node 50 between March 7, 2016 and March 14, 2016.**

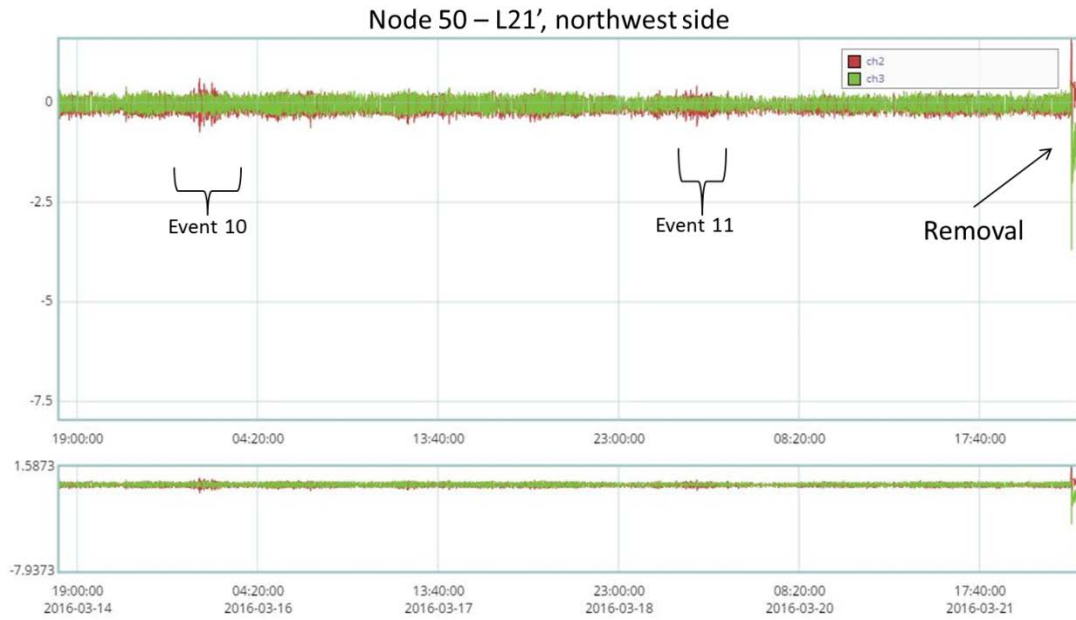


Figure 34: Data collected for Node 50 between March 14, 2016 and March 22, 2016.

#### A.4 Node 51

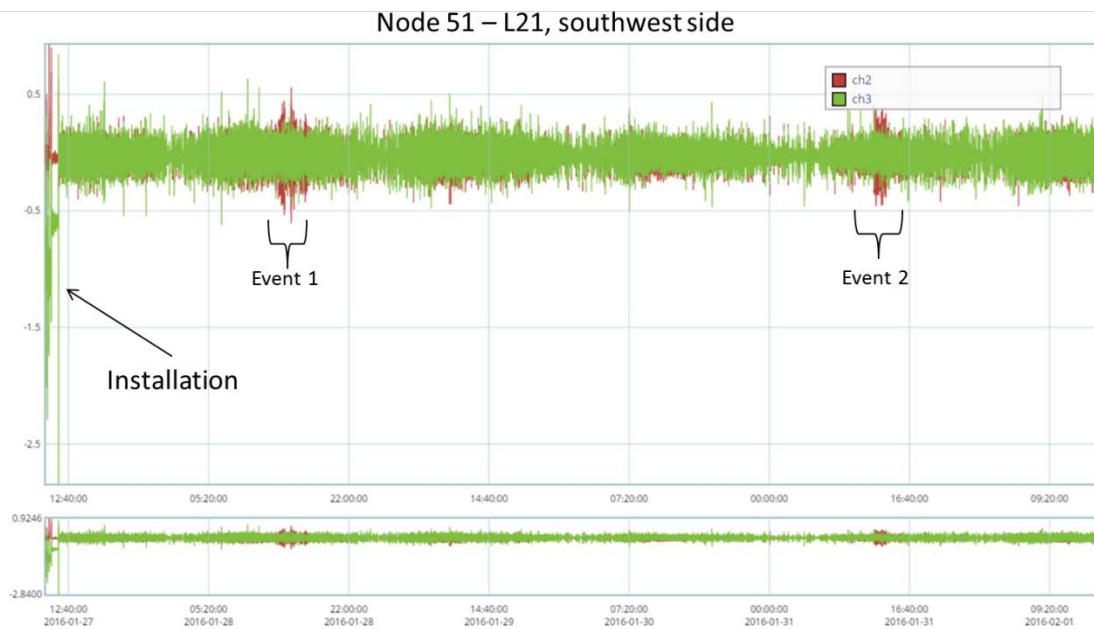


Figure 35: Data collected for Node 51 between January 27, 2016 and February 1, 2016.

Node 51 – L21, southwest side

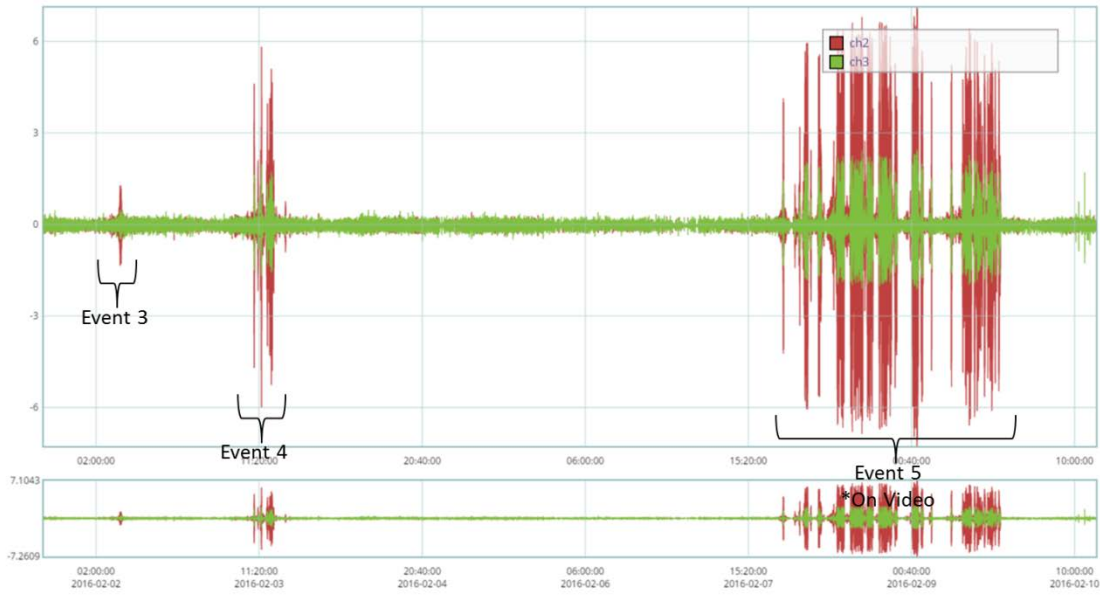


Figure 36: Data collected for Node 51 between February 1, 2016 and February 10, 2016.

Node 51 – L21, southwest side

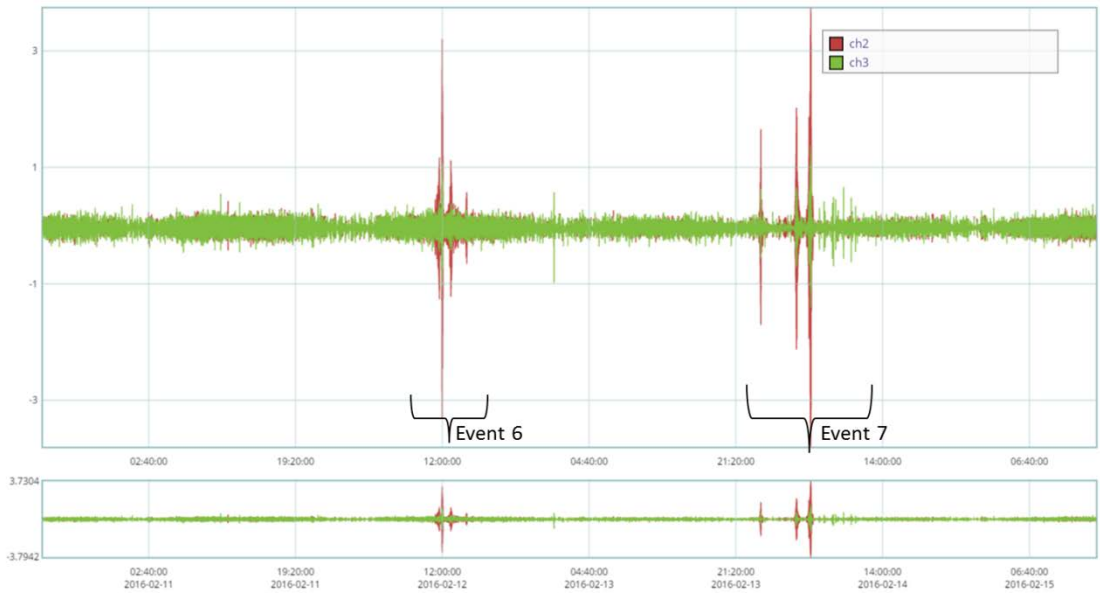
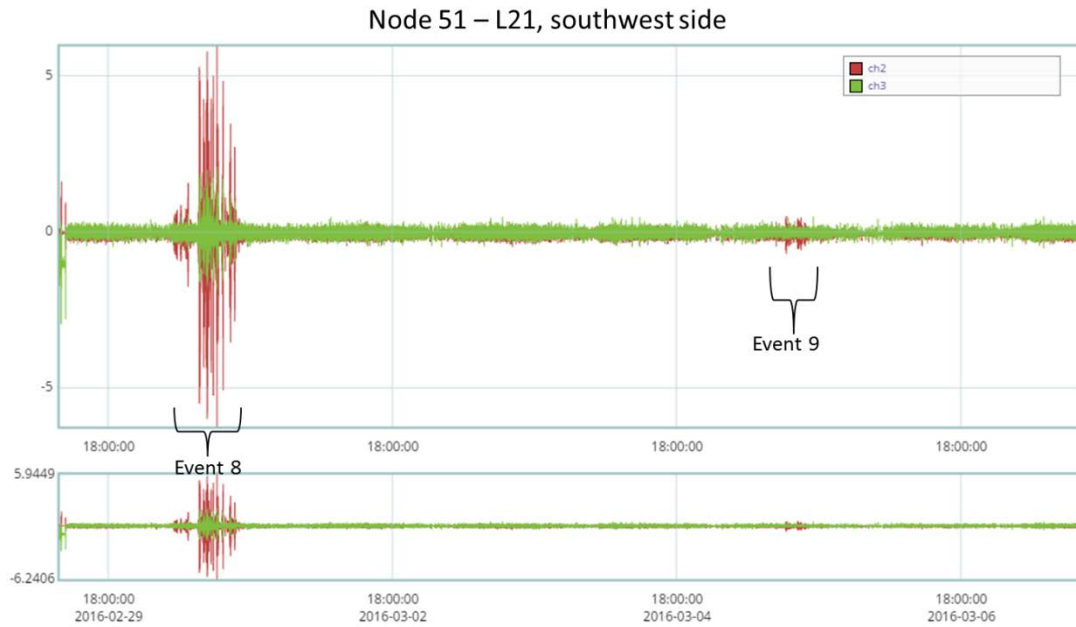
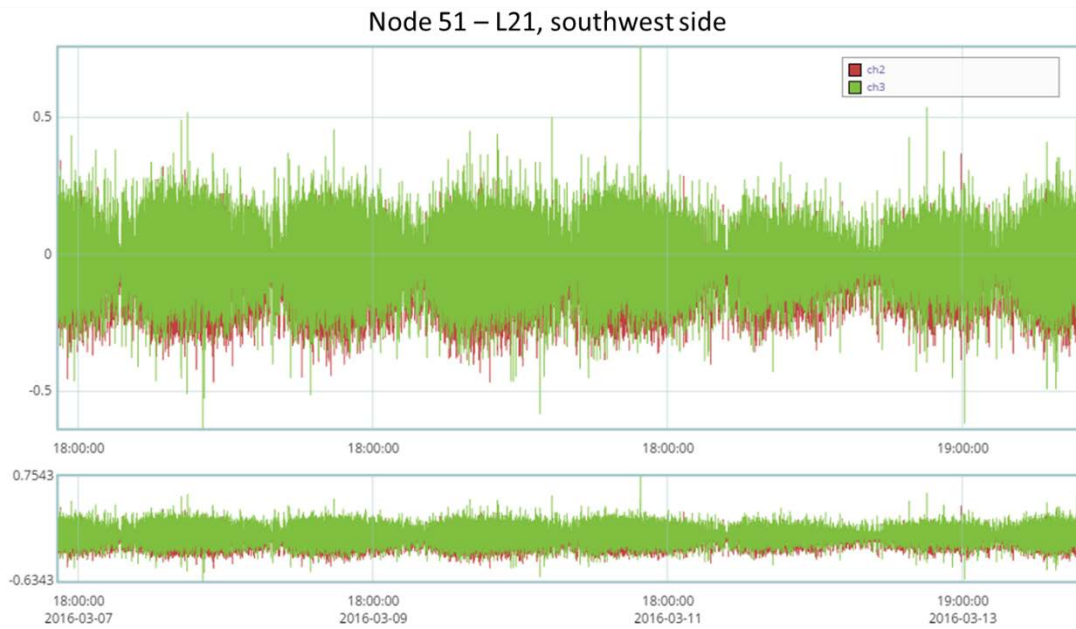


Figure 37: Data collected for Node 51 between February 10, 2016 and February 15, 2016.



**Figure 38: Data collected for Node 51 between February 29, 2016 and March 7, 2016.**



**Figure 39: Data collected for Node 51 between March 7, 2016 and March 14, 2016.**

Node 51 – L21, southwest side

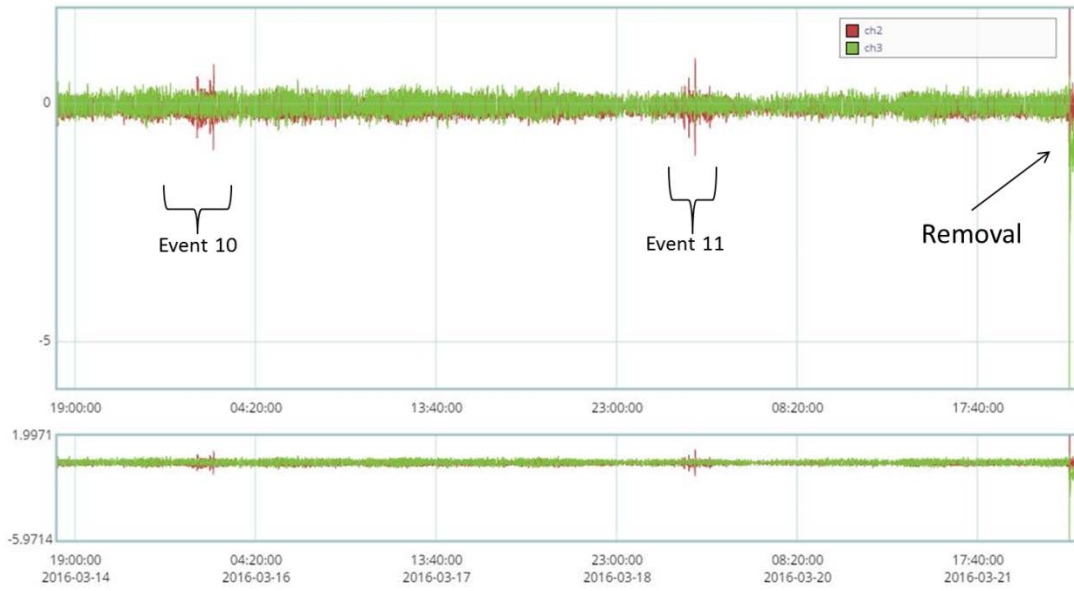


**Figure 40: Data collected for Node 51 between March 14, 2016 and March 22, 2016.**